Pharmaceuticals and personal care products removal from aqueous solution by nitrogen-functionalized carbon adsorbent derived from pomelo peel waste

Pharmaceuticals and personal care products removal from aqueous solution by nitrogen-functionalized carbon adsorbent derived from pomelo peel waste

P Prarat[1,*], K Hadsakunnee[2], L Padejepan[2], P Inlee[1], S Wongpaisan[1] and K Prasertboonyai[1]

1 Faculty of Science, Energy and Environment, King Mongkut's University of Technology North Bangkok (Rayong Campus), Rayong, Thailand
2 Department of Agro-Industrial, Food and Environmental Technology, Faculty of Applied Science, King Mongkut's University of Technology North Bangkok, Bangkok, Thailand
E-mail: panida.p@sciee.kmutnb.ac.th

Abstract. The aim of this work is to investigate the feasibility of the preparation of nitrogen-functionalized adsorbent material from waste pomelo peel by using diammonium hydrogen orthophosphate (DAP) activation for the removal of Pharmaceuticals and personal care products (PPCPs) such as carbamazepine (CBZ), clofibric acid (CFA) and oxytetracycline (OTC). Our results showed that the adsorbent prepared by chemical activation in the presence of DAP lead to mesoporous material. The adsorbent exhibits acid and basic groups at its porous surface. The kinetic data are found to follow a pseudo-second order kinetic model. The Langmuir model provided a good description of the experimental isotherms for CBZ, whereas CFA and OTC adsorption behavior rather follow the Freundlich model. Moreover, the PPCPs adsorption was found to be strongly dependent on the pH of solution as well as the pKa of both adsorbents and PPCPs. The strong adsorptive interaction between PPCPs and P-DAP was mainly attributed to the combination interactions of electrostatic interaction, hydrogen bonding and π-π interactions.

1. Introduction

In recent years, biologically active pharmaceuticals and personal care products (PPCPs) are among the most frequently detected environmental pollutants because PPCPs are extensively used in human and veterinary medicine, resulting in their continuous release to the environment. Even at low concentrations, PPCPs can cause the adverse effects on aquatic life and humans and has been suggested as an environmental micro-pollutant hazard. Therefore, the effective removal of PPCPs from water has become an increasingly important issue. Many studies have reported that most of the PPCPs are not biodegradable and often not easy to eliminate completely from water by biological and physical wastewater treatment plants due to their high polarity, aromaticity and structural complexity of these compounds [1, 2]. Consequently, other more effective treatment methods have been investigated, including chemical treatments such as ozonation [3], electrochemical degradation [4], and advanced oxidation process [5]. However, some of these intermediate compounds produces residual toxic compounds which are suspected to be more toxic than the parent compounds.

Adsorption is now recognized as an effective technique for pollutants removal because of its flexibility in implementation, high quality treatment outcomes, and the possibility of reusing the spent adsorbent. Activated carbon (AC) is preferred adsorbent for the removal of micropollutants from wastewater because of its high surface area, well-developed porosity and rich surface chemical functional groups. However, in recent years, the industrial production of AC is facing the problem of raw material scarcity and high costs. To decrease treatment costs, attempts have been made to find inexpensive alternative precursors for carbon preparation, such as organic waste products. AC derived from organic sources have a large specific surface area, mesoporous to microporous characteristics and high adsorption performance. One of these were carbon material form pomelo peel (PP) , which has a well-designed 3D structure with large pore size [6]. This structure can provide large active surface area and fast diffusion path, so carbon adsorbent produced from pomelo peel has been used for the adsorption of organic compound from solution; such as anionic and cationic dyes [7], and antibiotic [8].
The adsorption performance of carbon material depends on not only its surface area and pore structure, but also functional groups on its pore surface. According to literature, the oxygen-containing groups on AC play a key role on the adsorption process of pollutants. As a result, chemically activation agents (such as H_3PO_4, KOH, NaOH and $ZnCl_2$) have been frequently used for chemical activation due to the rich of the oxygen-containing groups on carbon adsorbent surface. However, the amino functional groups, as well as hydroxyl functional groups, play a significant role in the field of PPCPs adsorption [9]. Nevertheless, there was rare work to prepare nitrogen-functionalized activated carbon from agricultural wastes.
The aim of this study, di-ammonium hydrogen orthophosphate; $(NH_4)_2HPO_4$, was selected as the activation agent and pomelo peel waste was used as precursor material. Ammonium phosphates release phosphoric compound and amino radicals in the process of thermal decomposition, eventually promoting the porosity and surface amino functionalization of the produced activated carbon. After the preparation and the characterization of the adsorbent prepared, the removal of representative PPCPs, three drugs named carbamazepine (CBZ), clofibric acid (CFA) and oxytetracycline (OTC), by adsorption from aqueous solution was investigated. The characteristic and chemical structure of CBZ, CFA and OTC are summarized in table 1.

2. Materials and methods

2.1. Preparation of activated carbon

Pomelo peel (precursor) used for preparation of activated carbon were obtained locally. The precursor was first washed with distilled water, cut, dried, and sieved to desired mesh size of 3–4 mm. After soaking in DAP solution at a ratio of 1:3 (g precursor/g activate reagent) for 24 h, the sample was washed with distilled water until the pH was nearly neutral, and then dried at 105 ℃. After that, the sample was heated at temperature of 800 ℃ and hold at the carbonization temperature for 1 h. Finally, the produced carbon adsorbent (designated P-DAP) was ground, sieved and kept in a desiccator until use.

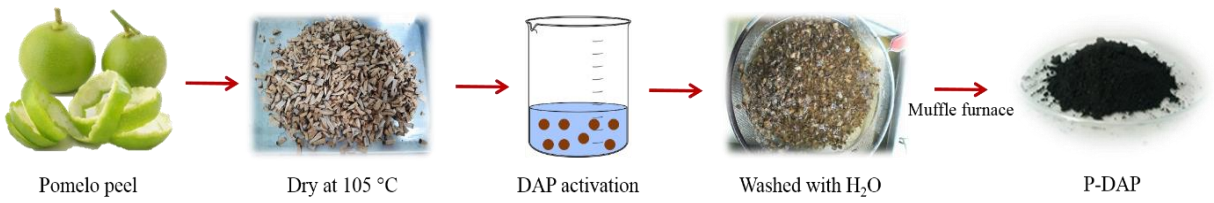

Figure 1. Schematic illustration of the N-functionalized activated carbon preparation.

2.2. Characterization of activated carbon

The physiochemical characteristics of P-DAP were characterized by several techniques. N_2 adsorption-desorption isotherms were analyzed with a V-Sorb 2800P surface area and pore volume

analyzer at 77 ℁. X-ray powder diffraction (XRD) patterns were obtained on a Bruker AXS D8 diffractometer using Cu-Kα radiation. The adsorbent was determined the pH at the point of zero charge (pH_{PZC}) by the acid-base titration method [10]. Fourier transform infrared (FT-IR) spectrophotometry was recorded on a Perkin Elmer Spectrum One using KBr pellets. Elemental analysis was carried out using a LECO Corporation, 628Series. Boehm's titration was carried out according to the Boehm's method [11].

2.3. Adsorption experiments

Batch adsorption experiment was studied in 125-ml Erlenmeyer flask containing 0.57 g/L of carbon absorbent. The solution pH and ionic strength was controlled by using a 10 mM phosphate buffer. The experimental samples were conducted with shaking condition at 200 rpm at room temperature, and then filtered through a glass filter (GF/C, pore size 0.45 μm). The quantity of CBZ, CFA and OTC concentration in equilibrium solutions was analyzed by a UV-Vis spectrophotometer (Shimadzu, UV 1800) at 275, 274 and 278 nm, respectively. The uptake capacity at the equilibrium q_e (mg/g) was calculated as follows:

$$q_e = \frac{(C_0 - C_e)V}{m} \tag{1}$$

where C_0 and C_e (mg/L) are the initial and equilibrium concentrations, respectively; V (L) is the volume of the solution; and m (g) is the dosage of the adsorbent.

Adsorption kinetic, the experiment was performed by fixing the initial three PPCPs concentration at 50 mg/L. Adsorption isotherm was performed at the concentration of PPCPs varied between 5 mg/L and 60 mg/L. While the effect of the pH on the adsorption capacity was investigated at pH range from 5 to 9. All the experimental samples were performed in duplicate, and the average values are reported.

2.4. Data analysis

The kinetics of the adsorption process were determined using the pseudo-first order and pseudo-second order kinetic models, as indicated in the Equation (2) and (3), respectively as follows:

$$log\ (q_e - q_t) = \log q_e - \frac{k_1}{2.303} t \tag{2}$$

$$\frac{t}{q_t} = \frac{1}{k_2 (q_e{}^2)} + \frac{t}{q_e} \tag{3}$$

where q_e and q_t (mg/g) are the adsorption capacities of adsorbate at equilibrium and at time, respectively. The k_1 and k_2 are the pseudo-first-order (1/min) and pseudo-second order rate constants (g/mg.min), respectively.

Langmuir and Freundlich isotherm models were investigated the adsorption process in this work. The Langmuir and Freundlich equation can be represented by the Equation (4) and (5), respectively as follows:

Langmuir isotherm

$$\frac{1}{q_e} = \frac{1}{K_L q_m} . \frac{1}{C_e} + \frac{1}{q_m} \tag{4}$$

Freundlich isotherm

$$\ln q_e = \frac{1}{n} \ln C_e + \ln K_F \tag{5}$$

where q_m (mg/g) is a theoretical maximum adsorption capacity, K_L (L/mg) is Langmuir isotherm constant, C_e is an equilibrium concentration (mg/L), K_F (L/mg) and n are Freundlich isotherm constant and heterogeneity factor indicating the adsorption intensity of the adsorbent, respectively.

Table 1. Characteristic and chemical structure of representative PPCPs.

Name	Molecular weight (g/mol)	pKa_1	pKa_2	pKa_3	Chemical structure
Carbamazepine (CBZ)	236.27	13.90	-	-	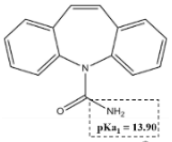
Clofibric acid (CFA)	214.65	3.61	-	-	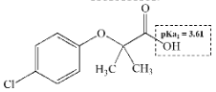
Oxytetracycline (OTC)	460.43	3.22	7.46	8.94	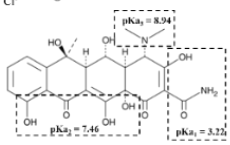

3. Results and discussion

3.1. Adsorbent Characterization

Figure 2a shows the N_2 adsorption/desorption isotherms and pore size distributions. The isotherms are mixture of type I and type IV with hysteresis loops, indicating the co-existence of micropores and mesopores. The mean pore size of P-DAP is 4.03 nm and a larger portion of mesoporous located in 20 nm (figure 2a and table 2). The BET surface area of P-DAP is 83.79 m^2/g which was lower than the other biomass activated carbons prepared under the similar activation agent. Guo et al. [12] has reported on the characteristic of carbon prepared from *Phragmites australis* by impregnating with DAP; denoted as AC-DAP. The BET surface area of AC-DAP was 495 m^2/g which was higher 5.6 times than that of P-DAP. However, the higher degree of mesoporosity is similarly present (>65%).

FT-IR spectroscopy was used to identify the major functional groups of the adsorbent (figure 2b. The peak at 3470 cm^{-1} can be assigned to the O–H stretching vibration of the hydroxyl groups, due to the existence of cellulose and lignin [13]. The peak at 2930 cm^{-1} indicates the C-H stretching in methyl and methylene groups [14].The presence of peak at 1662 cm^{-1} is characteristic of the C=O stretching in carboxyl group. The peak at 1385 cm^{-1} could be ascribed to phenolic C–O and O–H stretching modes. A small peak at 1034 cm^{-1} could result from ionized linkage P^{+}–O^{-}in phosphates and to symmetrical vibration in a chain of C–O–P [15] or C-N.

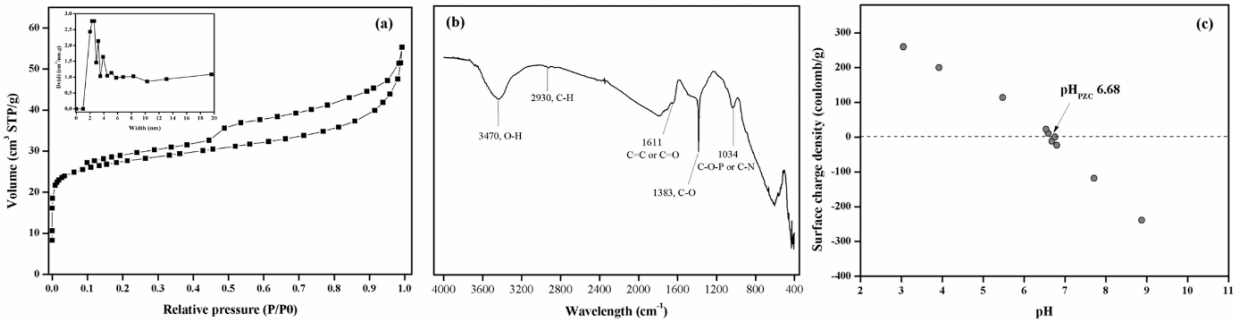

Figure 2. (a) Nitrogen adsorption/desorption isotherms with inset of pore size distribution, (b) FT-IR, and (c) surface charge density at various pH of solution and pH_{PZC} of P-DAP.

The point of zero charge (pH_{PZC}) of P-DAP is 6.68 as shown in figure 2c. This result indicates that the material is basic in nature due to the ammonium produced by DAP decomposition in activation process. Surface oxygen-containing groups of P-DAP determine its surface acidity/basicity, and act as a crucial factor affecting its adsorption capacity and selectivity. As shown in table 3, the result of Boehm titration showed that the amount of acidic and basic groups covering the surface of P-DAP. The contents of C H, N, O compositions (C, H, N, O and others) are 53.6%, 2.8%, 2.1% and 41.5%, respectively.

Table 2. Structural properties of P-DAP.

Adsorbent	S_{BET} (m^2/g)	Pore diameter (nm)	V_{total} (cm^3/g)	$V_{micropore}$ (cm^3/g)	$V_{mesopore}$ (cm^3/g)
P-DAP	83.79	4.03	0.08	0.02	0.06

Table 3. Surface functional groups and elemental composition of P-DAP.

Adsorbent	Acidic (mmol/g)	Basic (mmol/g)	Phenolic(mmol/g)	Carboxyl (mmol/g)	Lactone (mmol/g)	C (wt%)	H (wt%)	N (wt%)	O and others (wt%)
P-DAP	23.25	21.75	14.30	2.85	6.90	53.6	2.8	2.1	41.5

3.2. Adsorption kinetic

The kinetic profiles for the adsorption are presented in figure 3a and indicates that for three PPCPs adsorption took place via multi stages namely – a fast adsorption uptake that occurred within 2 h for both CBZ and CFA, followed by a slower, incremental uptake step with equilibrium reached within 8 h. Whereas with OTC adsorption, it took for long time and tended toward it at 30 h and was half maximal at ~6 h. The adsorption capacity rapidly increased in the initial stage due to the presence of number of available active sites for adsorption during the initial stages. The kinetic parameters and correlation coefficients are shown in table 4. For all three PPCPs the pseudo-second order model gave a better fit to the data (figure 3b and 3c), as defined by the higher R^2, than the pseudo-first order model. This result also exhibited that different adsorption mechanisms are involved in the adsorption process including chemical and physical adsorption, while the physical adsorption dominated in the adsorption process [16]. The adsorption mechanism on adsorbent surface should be proportional to the driving force and area. In this study, the driving force is the adsorbate concentration in the solution, and the area is the amount of active sites on the adsorbent surface.

Table 4. Kinetic parameters of CBZ, CFA and OTC.

PPCPs	$q_{e,exp}$	Pseudo-first order model			Pseudo-second order model		
		$q_{e,cal}$ (mg/g)	k_1 (min^{-1})	R^2	$q_{e,cal}$ (mg/g)	k_2 (g/mg.min)	R^2
CBZ	78.94	38.90	0.0049	0.9733	79.37	0.0126	0.9980
CFA	28.63	5.95	0.0007	0.5986	28.76	0.0025	0.9999
OTC	48.99	55.11	0.0002	0.8734	50.76	0.0197	0.9505

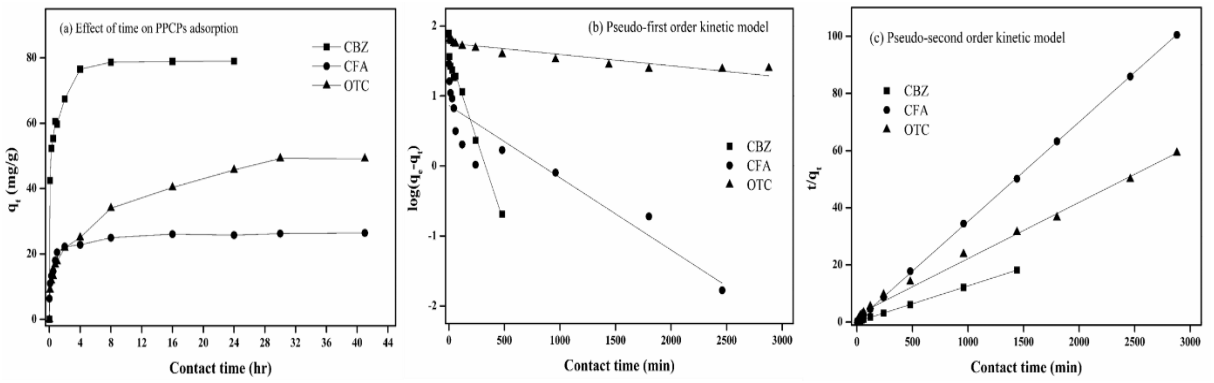

Figure 3. (a) adsorption kinetic of CBZ, CFA and OTC onto P-DAP, (b) Pseudo-first order kinetic model fitting, and (c) Pseudo-second order kinetic model fitting

3.3. Adsorption isotherms

Langmuir and Freundlich adsorption models were used to fit the experimental data. The adsorption model parameters are listed in table 5. Both the Langmuir and the Freundlich models fitted the three PPCPs isotherms well on the P-DAP, however, the exponent 1/*n* value for CFA and OTC was fairly less than half in the Freundlich models, which means that the form of the CFA and OTC adsorption equilibrium on P-DAP was more Freundlich like than Langmuir model. The results suggested that CFA and OTC adsorption behavior on P-DAP was not an ideal monolayer adsorption and the adsorption on the surface and pore of P-DAP were heterogeneous. While the value of 1/*n* of CBZ was more than 0.5, which implied that the actual data of CBZ adsorption can be described by the Langmuir model indicating that the monolayer chemisorption of CBZ on P-DAP was predominant.

Comparison on the effects of the different molecular structure of three PPCPs on adsorption capacities is shown in figure 4. P-DAP adsorbed the CBZ far more effectively than OTC and CFA. As revealed in figure 2d, the surface charge of P-DAP exhibited a nearly neutral at pH 7. Similarly, CBZ is neutral form (pK_a =13.90), whereas with CFA is anionic form (pKa = 3.61) and OTC are zwitterionic form, consequently P-DAP could adsorb CBZ via H-bonding interaction due to hydroxyl groups (pKa ~ 9.32) as well as amino groups (pKa ~ 9.6) on its surface. Moreover, CBZ can be adsorbed onto P-DAP due to the dispersive interactions between the delocalized π electrons in the P-DAP basal planes and the free electrons (aromatic rings) in the CBZ molecule. Hence, the much higher CBZ adsorption capacity should be ascribed to the combination of H-bonding and π-π interaction. With respect to CFA, its anionic form at pH 7 could contribute to repulse electrostatic interactions towards $-COO^-$ groups (pKa ~ 4.5) of P-DAP. For OTC adsorption, the zwitterion (H_2OTC and $HOTC^-$) was the major form at pH between 3.22 and 7.46, thus P-DAP could adsorb OTC by electrostatic interaction between H_2OTC and the weakly negatively charged P-DAP, including π-π interaction and H-bonding.

A comparison of the surface area and maximum PPCPs adsorption capacities per square meter (q_{max}, mg/m^2) of the P-DAP with other carbonaceous adsorbents is shown in table 6. Surprisingly, P-DAP exhibited lower surface area but obviously higher CBZ, CFA, and OTC adsorption capacities per square meter than other carbons. Accordingly, it can be mention that the excellent actual adsorption behavior due to organic functional group notably surpasses the influence of specific surface area of adsorbent as the P-DAP has a much lower surface area than the other adsorbents.

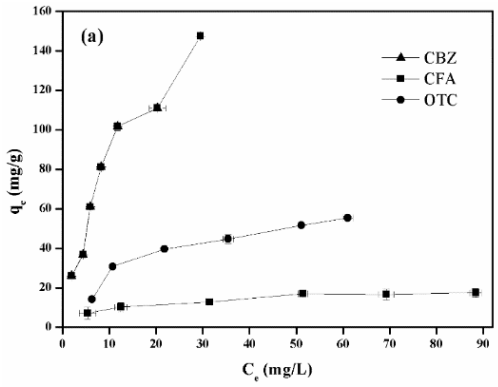

Figure 4. Adsorption isotherm of CBZ, CFA and OTC onto P-DAP at pH 7.

Table 5. Isotherm parameters of CBZ, CFA and OTC.

PPCPs	Langmuir			Fruendlich		
	q_m (mg/g)	K_L (L/mg)	R^2	K_F (L/mg)	$1/n$	R^2
CBZ	216.2	0.065	0.998	22.1	0.56	0.997
CFA	19.4	0.092	0.997	4.6	0.31	0.998
OTC	64.9	0.064	0.999	13.3	0.32	0.997

3.4. Effect of pH on PPCPs adsorption capacity

In figure 5, CBZ adsorption capacity was higher under neutral pH than that at acidic and basic pH. The pKa of CBZ is around 13.90, so it maintained neutral molecular (figure 6a) form throughout the investigation. The H-bonding and π-π interactions were responsible for the adsorption of CBZ. When the pH increase, the density of the negative surface charge at pH 9 of the P-DAP was higher than that at pH 5 and 7, leading to a lower adsorption capacity.

On the contrary, increasing the pH resulted in a lower CFA and OTC adsorption on P-DAP. As the pKa of CFA is 3.61, it exists in anionic form (figure 5b). The surface of P-DAP carbon is more positive charge at pH = 5, which is at a pH lower than its pH_{PZC}. Therefore, the higher adsorption capacity of CFA on P-DAP at low pH may be consequent on the electrostatic interaction between the positively charged surface of P-DAP and the CFA anions. With the increase in pH, the adsorption capacity decreased, which may be explained by the repulsive electrostatic interaction between P-DAP and the CFA anions. Moreover, the maximum uptake of OTC is obtained at pH = 5 and the adsorption decreased at higher pH, with reflects the unfavorable electrostatic conditions for anionic OTC molecules and negatively charged P-DAP.

Table 6. Surface area and maximum CBZ, CFA and OTC adsorption capacities per square meter of the various carbonaceous materials.

Adsorbents	BET (m^2/g)	q_{max} (mg/g)	q_{max} (mg/m^2)			Reference
			CBZ	CFA	OTC	
Commercial GO (type C)	771	CBZ = 195	0.253			[17]
Commercial GO (type M)	74	CBZ = 19	0.257			[17]
CNT	112	CBZ = 28	0.250			[17]
GAC	1181	CBZ = 297	0.251			[17]
Cotton liner fiber AC (CLAC)	2143	CBZ = 1025.2			0.478	[18]
Cotton cloth waste AC (ACC50%)	1175	CFA = 49.9 TC = 109.1		0.043	0.093	[19]
Commercial AC (CP)	907	CFA = 82.6		0.091		[20]
Commercial AC (VP)	758	CFA = 101.7		0.134		[20]
P-DAP	83.79	CBZ = 216.2	2.579			This work
P-DAP	83.79	CFA = 19.4		0.231		This work
P-DAP	83.79	OTC = 64.9			0.775	This work

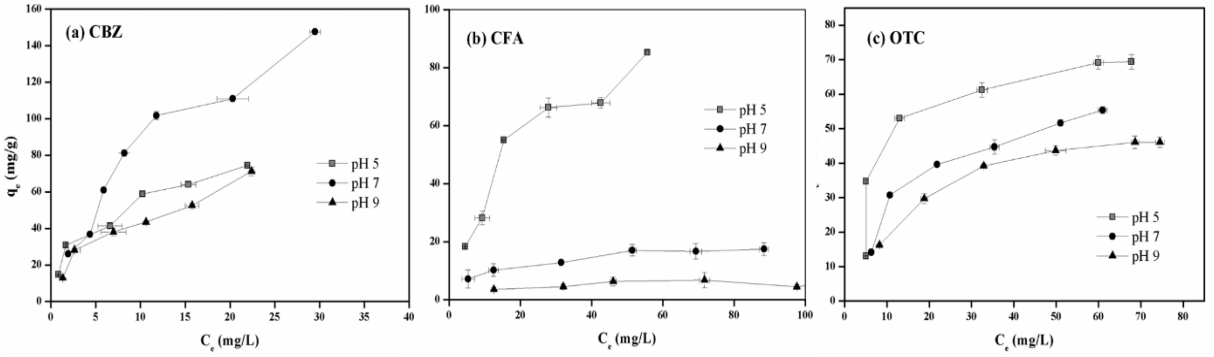

Figure 5. Effect of pH on adsorption of CBZ, CFA and OTC onto P-DAP.

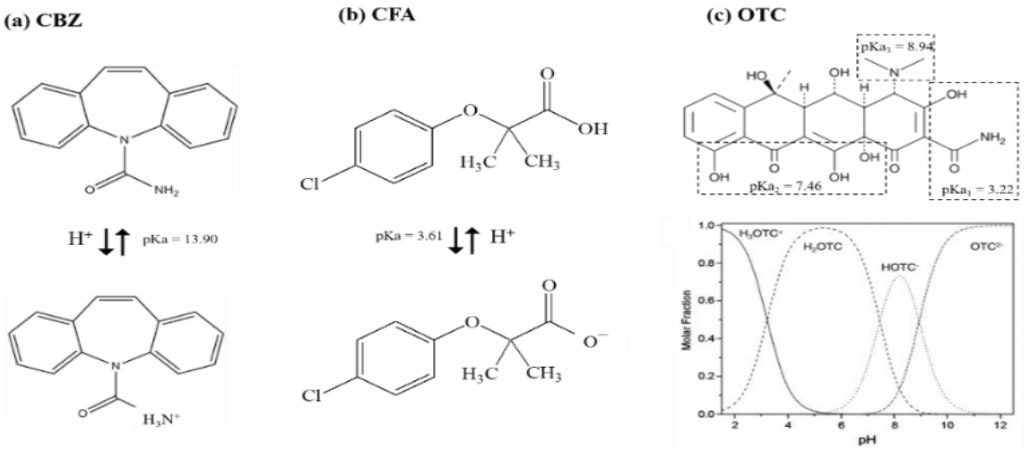

Figure 6. The pKa values of CBZ, CFA and OTC and pH-dependent speciation of OTC.

4. Conclusions

The liquid-phase adsorption of CBZ, CFA and OTC (three representative PPCPs) has been studied for the first time using nitrogen-functionalized carbon adsorbent derived from pomelo peel waste, the following conclusion can be drawn. P-DAP exhibited a high ratio of mesoporous structure (>70%), and contained the acid and basic groups at its porous surface. The Freundlich model appeared to fit the data better than the Langmuir model for describing the adsorption behavior of CFA and OTC with the exception of the equilibrium data of CBZ that is well described by the Langmuir model. The electrostatic interaction, hydrogen bonding and π-π interaction played the key role influencing the PPCPs adsorption. Operating variables including adsorbent dose, PPCPs concentration, solution of pH and coexisting of natural organic matter will be optimized using central composite design (CCD) under response surface methodology (RSM) approach in further studies.

5. References

[1] Chen Y, Vymazal J, Březinová T, Koželuh M, Kule L, Huang J and Chen Z 2016 *Sci. Total Environ.* **566-567** 1660-69
[2] Zhang D, Gersberg R M, Ng W J and Tan S K 2014 *Environ. Pollut.* **184** 620-39
[3] Coelho A D, Sans C, Agüera A, Gómez M J, Esplugas S and Dezotti M 2009 *Sci. Total Environ.* **407** 3572-78
[4] Joss A, Zabczynski S, Göbel A, Hoffmann B, Löffler D, McArdell C S, Ternes T A, Thomsen A and Siegrist H 2006 *Water Res.* **40** 1686-96
[5] Klavarioti M, Mantzavinos D and Kassinos D 2009 *Environ. Inter.* **35** 402-17
[6] Chen S, Liu Q, He G, Zhou Y, Hanif M, Peng X, Wang S and Hou H 2012 *J. Mater. Chem.* **22** 18609-13
[7] Foo K Y and Hameed B H 2011 *Chem. Eng. J.* **173** 385-390.

[8] Sun Y, Li H, Li G, Gao B, Yue Q and Li X 2016 *Bioresour. Technol*. **217** 239-44
[9] Li N, Yang S, Chen J, Gao J, He H and Sun C 2016 *Appl. Surf. Sci.* **386** 460-66
[10] Peng X, Hu X, Fu D and Lam F L Y 2014 *Appl. Surf. Sci.* **294** 71-80
[11] Boehm H P 1994 *Carbon* **32** 759-69.
[12] Guo Z, Fan J, Zhang J, Kang Y, Liu H, Jiang L and Zhang C 2016 *J. Taiwan Inst. Chem. Eng.* **58** 290-96.
[13] Liang S, Guo X and Tian Q 2011 *Desalination* **275** 212-16
[14] Zhang X, Niu J, Zhang X, Xiao R, Lu M and Cai Z 2017 *J. Chromatogr. B* **1046** 58-64
[15] Liu H, Zhang J, Bao N, Cheng C, Ren L and Zhang C 2012 *J. Hazard. Mater.* **235-236** 367-75
[16] Jung C, Heo J, Han J, Her N, Lee S J, Oh J, Ryu J and Yoon Y 2013 *Sep. Purif. Technol.* **106** 63-71
[17] Cai N, and Larese-Casanova P 2014 *J. Colloid Interface Sci*. **426** 152-61.
[18] Sun Y, Yue Q, Gao B, Li Q, Huang L, Yao F and Xu X 2012 *J. Colloid Interface Sci*. **368** 521-27
[19] Boudrahem N, Delpeux-Ouldriane S, Khenniche L, Boudrahem F, Aissani-Benissad F and Gineys M 2017 *Process Saf. Environ. Prot.* **111** 544-59
[20] Mestre A S, Nabi ço A, Figueiredo P L, Pinto M L, Santos M S C S and Fonseca I 2016 *Chem. Eng. J.* **286** 538-48

Acknowledgements
This research was funded by King Mongkut's University of Technology North Bangkok; Contract no. KMUTNB-62-KNOW-33. Moreover, we would like to thank Faculty of Science, Energy and Environment, King Mongkut's University of Technology North Bangkok (KMUTNB) for the equipment.